Aggregation of Telechelic Triblock Copolymers: From Animals to Flowers

D. Lairez,*,† M. Adam,†,‡ J.-P. Carton,§ and E. Raspaud†

Laboratoire Léon Brillouin, CEA-CNRS, and Service de Physique de l'Etat Condensé CEA Saclay, 91191 Gif-sur-Yvette Cedex, France

Received May 13, 1997; Revised Manuscript Received August 25, 1997[⊗]

ABSTRACT: We present an experimental study of dilute solutions of a polystyrene−polyisoprene−polystyrene block copolymer in a bad solvent of the polystyrene terminal blocks (heptane). At high temperature, it was previously shown that these copolymers associate in polydisperse and loose aggregates having a small association number and a large radius of gyration. These aggregates have been called "animals". Here, we deal with the change of the aggregate structure as the solvent selectivity is increased. Actually, scattering experiments show an aggregate compaction as the temperature is decreased. They pass from an "animal" to a "flowerlike" structure with a dense core and a swollen corona. However, small angle neutron scattering proves that these flowerlike micelles are always linked together. In addition, to account for this compaction, we present the study of a diblock copolymer, corresponding to roughly half of the triblock, and measurements of the solubility of homopolystyrene in heptane. This allows us to quantify the different terms of the free energy per chain in the aggregates, from which one perceives how the temperature tunes the balance of interfacial tension and conformational entropy leading to different aggregates conformations.

1. Introduction

Associating polymers are extensively studied (for a review article see ref 1). The simplest case is that of diblock copolymers in a selective solvent, i.e., copolymers made of two sequences of different chemical species A and B dissolved in a nonsolvent or bad solvent for the A species. Minimization of the interfacial energy between the solvent and the A blocks leads to copolymer association. Even in this simple case, many features of the aggregation of these copolymers remain unsolved, in particular for weak solvent selectivity.[2] However, for strong solvent selectivity, asymmetric diblock copolymers (the mass of the A block being smaller than the one of the B block) are known to form spherical micelles[3,4] which can be described using the star polymer model.[5] The understanding of multiblock copolymers is another important challenge as they are often encountered in many biological systems.[6,7] From a theoretical point of view, the difference between diblock and multiblock copolymers was already pointed out, in particular, their ability to bridge, leading to macrophase separation.[8] Telechelic triblock copolymers dissolved in a bad solvent of the terminal blocks is the simplest case which can be considered. Theoretical predictions concerning the structure of the aggregates is quite controversial. Some authors do not consider fundamental differences between the aggregation of di- and triblocks, the latter leading to flowerlike structure.[8,9] Following others, the entropy loss needed for the two terminal blocks to join together prevents triblocks to form this kind of micelles.[10] Computer simulations[11] have shown that the structure depends on the energy balance between the entropy loss and the interfacial tension gain, i.e., solvent selectivity.

In a previous paper,[12] experimental results concerning dilute solutions of polystyrene−polyisoprene−polystyrene in a bad solvent (heptane) of the polystyrene were reported. It was shown that at high temperature (50 °C) triblock copolymers associate in polydisperse and loose aggregates having a small association number and a large radius of gyration. These aggregates will be called "animals"[13] in the following. This paper is devoted to the study of the change in the aggregate structure as the temperature is decreased, i.e., as the solvent selectivity increases. In particular, as spherical micelles are often taken as a reference, a systematic comparison with a diblock copolymer, corresponding to roughly half of the triblock, will be done.

In the Experimental Results section, measurements of the solubility of homopolystyrene in heptane allow us to quantify the solvent selectivity. For the micellization of diblock copolymers, the temperature behavior of the association number is measured by light scattering. Small-angle neutron scattering experiments indicate a dense core and a swollen corona for these diblock micelles. As for triblock copolymers, experimental results obtained by light and neutron scattering give evidence for an aggregate compaction as the temperature is decreased. The aggregates pass from an "animal" to a "flowerlike" structure. However, small-angle neutron scattering proves that these flowerlike micelles are always linked together. Such triblock micelles association was expected theoretically[8,14] and already suspected experimentally[15,16] but has never been clearly shown. These micelle associations are precursors of the macroscopic phase which appears for even stronger solvent selectivity and which is responsible for the cloudy point often reported on these systems.[17] Finally, in the last part, a tentative confrontation between experiments and theory is done with particular attention to numerical values. Actually, for our copolymer/solvent systems, the use of results obtained on homopolystyrene and on diblock copolymers allow us to quantify the different energies involved in the triblock aggregate conformations.

2. Experimental Results

2.1. Sample Characteristics and Previous Results. The experiments reported here were performed

† CEA-CNRS.

‡ Present address: Institut Laue Langevin, BP156, 38042 Grenoble Cedex 9, France.

§ Service de Physique de l'Etat Condensé.

⊗ Abstract published in *Advance ACS Abstracts,* October 15, 1997.

S0024-9297(97)00666-9 CCC: $14.00

Table 1. Diblock and Triblock Copolymers Characteristics

	% of PS	M (g/mol)	$R_{g\ app}$ (Å)	R_H (Å)
diblock (in THF)	30	$(8.0 \pm 0.3) \times 10^4$	unmeasured	67 ± 3
Triblock (in THF or in heptane at high temperature)	21	$(1.30 \pm 0.05) \times 10^5$	205 ± 10	100 ± 5

on a triblock copolymer whose characteristics are comparable to the one studied in ref 12. It is a polystyrene−polyisoprene−polystyrene copolymer (PS−PI−PS) having a molecular mass equal to $M = (1.30 \pm 0.05) \times 10^5$ g/mol and a weight fraction of PS equal[18] to 21% ($M_{PS} \cong 2.7 \times 10^4$ g/mol and $M_{PI} \cong 1.03 \times 10^5$ g/mol). The experimental results obtained on these triblock copolymers are compared with results obtained on a diblock copolymer which corresponds to roughly half of the triblocks ($M = (8.0 \pm 0.3) \times 10^4$ g/mol, 30% PS, $M_{PS} \cong 2.4 \times 10^4$ g/mol and $M_{PI} \cong 5.6 \times 10^4$ g/mol). The characteristics of copolymers were determined by static and quasielastic light scattering measurements performed on samples diluted in a good solvent (THF) for the two polymer species and also at high temperature for the triblock copolymers. The measured quantities such as the scattered intensity per monomer, the apparent radius of gyration and the hydrodynamic radius were extrapolated to zero scattering angle and to zero concentration (see Table 1). For the study of the copolymer aggregation, heptane was used as a solvent, which is a bad solvent for the polystyrene blocks and a good solvent for the polyisoprene at any temperature.

In a previous paper,[12] using light (static and dynamic) and neutron scattering experiments, it was shown that at high temperature ($40 < T$ (°C) < 60) there is a critical aggregation concentration cac $= 1.5 \times 10^{-3}$ g/cm^3 above which triblock copolymers associate in polydisperse and loose aggregates with a small association number ($p < 10$) and large radius of gyration (up to 1500 Å). All the experimental results obtained in this first study are consistent with low density aggregates having presumably a branched conformation similar to the one of animals.[13] The following will often refer to this cac determined at high temperature, even if at low temperature aggregates having another conformation are observed below the cac.

2.2. Polystyrene Solubility Measurements. The heptane quality for polystyrene blocks depends on the temperature. In order to quantify this feature, the solubility of the PS having different molecular weights ($M = 7 \times 10^3$, 1.16×10^4, and 2.20×10^4 g/mol) were measured as a function of temperature between 30 and 80 °C. The molecular weight of polymers being known, their concentration in the dilute phase (saturated solution) was deduced from the scattered intensity I_q at fixed angle. Actually, neglecting the second virial coefficient and the polymer size, this concentration C_s is equal to

$$C_s = K\frac{I_{q\to 0}}{M} \cong K\frac{I_q}{M} \qquad (1)$$

where I is the intensity scattered by the polymer divided by the solvent scattered intensity measured independently at each temperature. The transfer vector q and the constant K are given by $q = (4\pi n/\lambda)\sin(\theta/2)$ and $K = \lambda^4 N_a R/(4\pi^2 n^2)(dn/dC)^2$, where θ, n, dn/dC, N_a, λ, and R are the scattering angle, the index of refraction, the index increment, Avogadro's number, the wavelength, and the solvent Rayleigh ratio, respectively. To perform these solubility measurements, filtered heptane was added to a large amount of polymers ($C > 5 \times 10^{-2}$ g/cm^3), the sample was slightly centrifuged in order to precipitate the dense phase and then heated up to the desired temperature. The measurements were performed once equilibrium scattered intensity was reached for increasing temperature. Figure 1 shows that for the sample having a molecular weight equal to the one of the PS precusor of the diblock copolymer ($M_{PS} = 2.20 \times 10^4$ g/mol), the solubility increases by a factor of 10 as the temperature increases by 20 °C. Depending on the PS molecular mass, measurements cannot be performed below a given temperature because the intensity scattered by the polymer is smaller than the experimental reproducibility (2%). In part 3.1, the temperature and molecular mass dependence of the solubility will be used to determine the PS/heptane interfacial tension which is the driving force of the aggregation process.

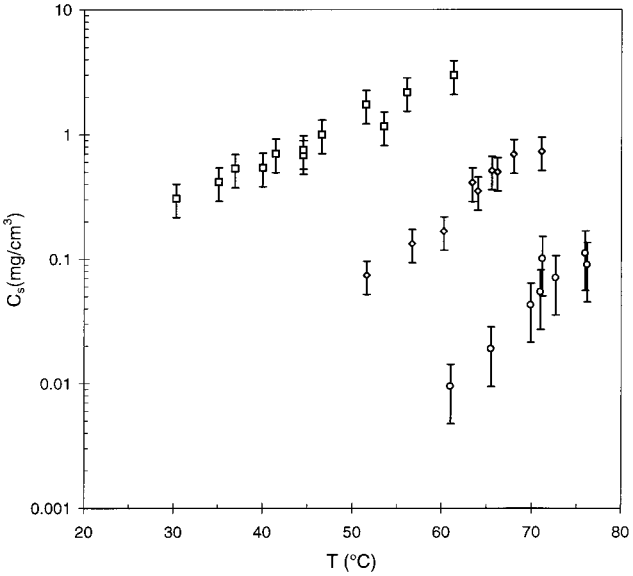

Figure 1. Temperature dependence of the solubility C_S of three homopolystyrene samples having masses equal to 7×10^3 (squares), 1.1×10^4 (diamonds) and 2.2×10^4 g/mol (circles), in heptane. Measurements were performed by static light scattering.

2.3. Light Scattering Measurements. Details of the light scattering apparatus as well as the data treatment have been fully described elsewhere.[19] The argon laser (wavelength $\lambda = 4880$ Å) is focused in the sample cell, which is placed in a vessel containing toluene and surrounded by a copper cylinder (high thermal conductivity). The base of the cylinder is in contact with a copper box in which thermostated water flows. A radial slit on the copper cylinder allows light scattering experiments to be performed at scattering angles θ ranging from 10 to 150°. The vertical thermal gradient measured at the center of the sample is less than 0.2 °C/cm.

2.3.1. Diblock Copolymers. Diblock copolymer aggregation was studied in heptane at concentrations between 3.8×10^{-6} and 8.9×10^{-4} g/cm^3. In the temperature range investigated (between 10 and 40 °C) diblock copolymers aggregate for concentrations higher than the cmc. At 20 °C, this cmc is so small that it cannot be determined with a good accuracy. The

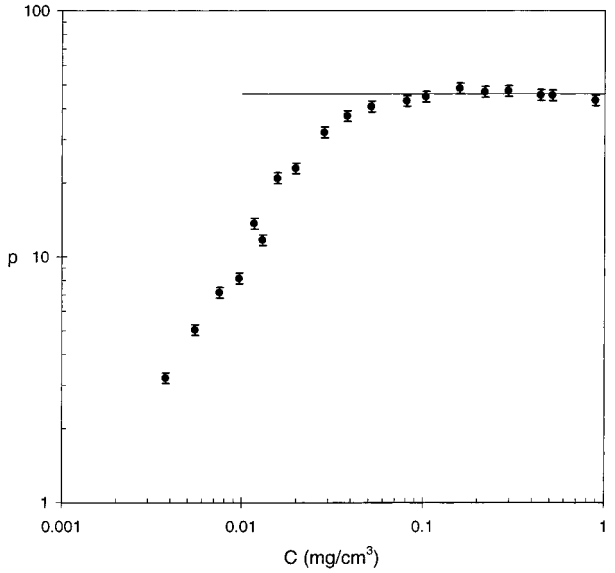

Figure 2. Diblock copolymer association number p as a function of the concentration *C*. Measurements were performed at $T = 22$ °C by static light scattering, the association number being deduced from the ratio of the absolute scattered intensity per monomer I/C extrapolated to zero transfer vector divided by the mass of free copolymers. The line corresponds to the mean value $p = 46 \pm 2$ measured for C between 10^{-4} and 8.9×10^{-4} g/cm^3.

molecular weight M, the apparent radius of gyration R_{gapp}, and the diffusion coefficient were measured by static and quasielastic light scattering. The association number p is taken as the ratio of the mass M_{agg} deduced from the scattered intensity per monomer I/C extrapolated to zero transfer vector, to the mass of free copolymers M_1.

$$p = \frac{M_{agg}}{M_1} \quad \text{with } M_{agg} = KI_{q\to 0}/C \tag{2}$$

In doing so, the effect of the second virial between aggregates is neglected. As the concentration of free copolymers still present in the solution is expected to be on the order of the cmc, their contribution to the scattered intensity is also neglected for the determination of the mass of the aggregates. The radius of gyration R_{gapp} determined by the q dependence of the scattered intensity at $qR_{gapp} < 1$ is apparent and differs from the actual radius of gyration because of the difference of refractive index increment between PS and PI. In order to calculate the actual radius of gyration R_g, the conformation of the aggregates should be known. In the following one must be aware of a proportionality factor between R_g and R_{gapp} which depends on the conformation.[20,21]

In Figure 2, the association number p measured at $T = 22$ °C is plotted as a function of the concentration. The association number increases as the concentration increases from 3.8×10^{-6} up to 10^{-4} g/cm^3 and then reaches a constant value $p = 46 \pm 2$ for concentrations between 10^{-4} and 8.9×10^{-4} g/cm^3. In the concentration range for which the association number is constant, the apparent radius of gyration is found to be equal to $R_{gapp} = 205 \pm 5$ Å. The hydrodynamic radius R_H is deduced from the diffusion coefficient D determined from quasielastic light scattering measurements: $R_H = kT/(6\pi\eta_0 D)$, where η_0 is the solvent viscosity. It is found to be $R_H = 290 \pm 5$ Å.

Diblock copolymers aggregates present a high association number and a small radius of gyration compared to triblock copolymer aggregates at high temperature (see ref 12 and section 2.3.2). The experimental values given above imply a high internal concentration (on the order of 10%). At concentrations higher than 8.9×10^{-4} g/cm^3, the overlap concentration is approached and the light scattered intensity per monomer extrapolated to zero q decreases due to strong interactions between aggregates, but it remains always higher by a factor 10 than the one of free copolymers. However, in the same concentration range, the scattered intensity becomes q independent. This is an indication of a scattered intensity maximum at higher q due to strong interactions as for star polymers[22] and spherical micelles.[4] Both the high internal concentration and this type of interaction argue in favor of dense aggregates as spherical starlike micelles. Another argument supporting this conformation concerns the ratio of the radius of gyration of the aggregate to the one of free diblock micelles. For starlike polymers, this ratio is expected[23] to increase with the number f of arms as

$$\frac{R_g}{R_{garm}} = f^{(1-\nu)/2} \tag{3}$$

$\nu = 0.588$ being the excluded volume exponent and R_{garm} the radius of gyration of a linear polymer in a good solvent having the same mass as the arm of the star polymer. For diblock copolymers, only apparent radii of gyration are measured. In addition, since the relation between the actual and the measured radii of gyration depends on the copolymer conformation, let us assume a ratio $(R_g/R_H)_{micelles} = (3/5)^{1/2}$ as for spheres and a ratio $(R_g/R_H)_{free\ diblocks} = 1.56$ as for swollen linear polymers. The measured values of the hydrodynamic radii (see the Table) lead to $(R_{g\ micelles}/R_{g\ free\ diblocks}) = 2.15 \pm 0.15$, in agreement with the power 0.2 of the association number ($(46 \pm 2)^{0.2} = 2.15 \pm 0.02$). The spherical starlike structure for diblock copolymer micelles will be confirmed by small angle neutron scattering measurements reported in section 2.4.

In Figure 3 the association number p measured for concentrations between 2.0×10^{-5} and 6.7×10^{-4} g/cm^3 is plotted as a function of temperature. The increase of the association number with decreasing temperature is a direct consequence of the increase of the solvent selectivity reported in section 2.1. While at high temperature p is found to be strongly concentration dependent, at low temperature a concentration-independent behavior is found. The concentration dependence of p at high temperature can be interpreted as being due to a shift to higher concentrations and smaller association numbers of the curve in Figure 2 as the temperature is increased. The concentration independent behavior at low temperature is compatible with the full line corresponding to the theoretical variation of p expected from the polystyrene solubility measurements (see part 3).

2.3.2. Triblock Copolymers. The first characteristic feature is that, contrary to diblock copolymers, triblock dilute solutions become cloudy as the temperature is decreased. For example, the intensity scattered by a diblock copolymer solution at a concentration of $C = 4.6 \times 10^{-4}$ g/cm^3 increases only by a factor 1.2 as the temperature decreases from 20 to 10 °C, while for triblock copolymer solution at $C = 5.3 \times 10^{-4}$ g/cm^3, the scattered intensity apparently diverges at a tempera-

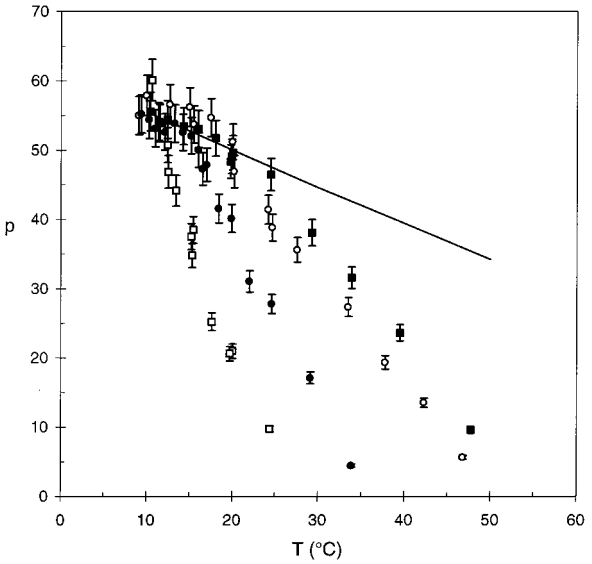

Figure 3. Diblock copolymer association number p measured by light scattering as a function of temperature. The symbols correspond to different concentrations (C in g/cm^3): 2.0×10^{-5} (open squares), 6.7×10^{-5} (full circles), 4.7×10^{-4} (open circles), and 6.7×10^{-4} (full squares). The increase of p with decreasing T reflects the increase of the solvent selectivity. The line corresponds to the variation of p which is expected from the PS precursor solubility measurements (see section 3.2).

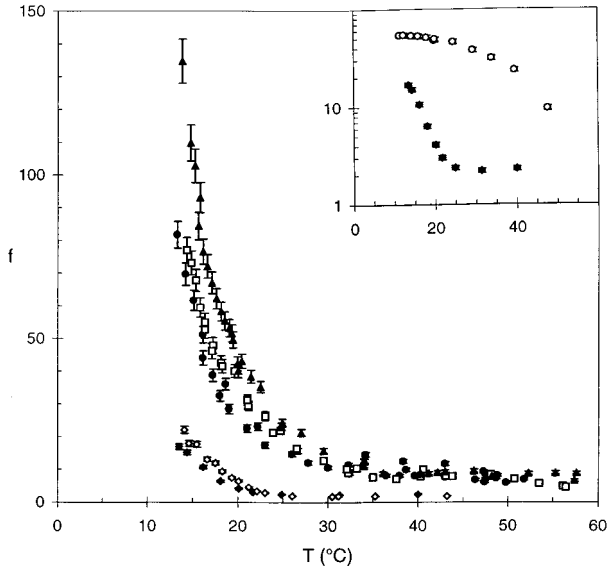

Figure 4. Temperature dependence of twice the association number of triblock aggregates ($f = 2p$ corresponds to the number of PS blocks per aggregate) which is compared to the diblock association number in the inset. The symbols correspond to different concentrations for triblock: full triangles, 6.7×10^{-3}; open squares, 3.0×10^{-3}; full circles, 1.7×10^{-3}; open diamonds, 8.9×10^{-4}; full diamonds, 5.3×10^{-4}. For diblock: open circles, $C = 4.7 \times 10^{-4}$ g/cm^3.

ture $T_d = 11$ °C. This increase of the scattered intensity is interpreted as being due to the formation of a two-phase system. The temperature T_d at which this phase separation occurs, increases slightly with the concentration: at a concentration of 10^{-2} g/cm^3 it is on the order of 15 °C. Note that once this demixion occurs, a hysteresis is observed when the temperature is increased from T_d. However, the following results are obtained as the temperature is decreased from 40 °C to T_d and then increased, to ensure that only reversible data are reported.

For triblock copolymers at temperature above T_d, five concentrations were studied, three of them being higher than the cac and two of them being smaller. The molecular weight M, the apparent radius of gyration R_{gapp}, and the diffusion coefficient were measured as a function of the temperature, between 50 °C and T_d. As for diblock copolymers, the contribution of free copolymers still present in the solution is neglected for the calculation of the association number. This approximation is not valid at high temperature ($T > 40$ °C). It has been shown[12] that the concentration of free copolymers increases with the total concentration and that their scattered intensity has to be taken into account, for an exact determination of the association number.

In Figure 4, twice the association number p is plotted as a function of the temperature for triblock copolymers. One can see that it increases by more than one decade as the temperature is decreased from 30 to 13 °C. In this low-temperature range, the association number depends on the concentration. This dependence could be interesting, however this is not the purpose of this paper. To compare di- and triblock aggregation, in the inset of Figure 4, the number f of PS blocks per aggregate is plotted as a function of the temperature. For diblock copolymer micelles the association number p is equal to f, while for triblock copolymers one has $f = 2p$. At the same concentration, f is always larger for diblock than for triblock copolymers. However, the

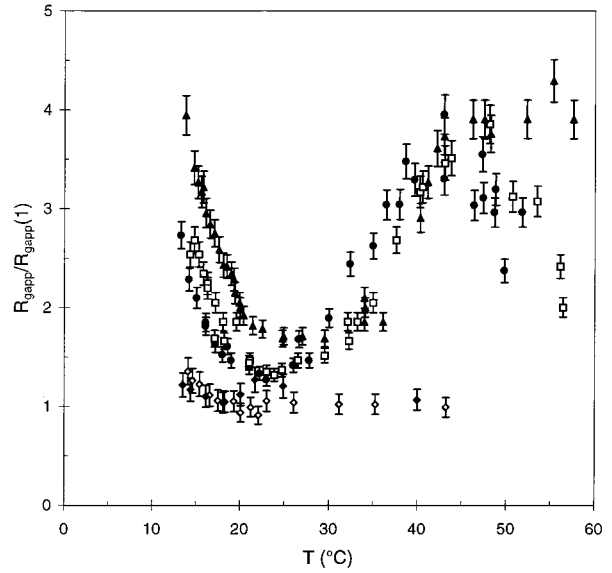

Figure 5. Variation of the reduced apparent radius of gyration $R_{gapp}(p)/R_{gapp}(1)$ as a function of temperature T (°C) for triblock copolymers. $R_{gapp}(p)$ is the apparent radius of gyration of aggregates having an association number of p and $R_{gapp}(1)$ is one of the free triblock copolymers (see Table 1). Symbols have the same meaning as in Figure 4.

increase of f for decreasing temperature is smaller for the diblock than for the triblock. In addition, note that increasing the concentration leads to a triblock association number higher than the one of diblocks which is concentration independent at low temperature (see Figure 3).

The most striking result is the variation of the apparent radius of gyration with temperature (see Figure 5). For the three highest concentrations ($C >$ cac) as the temperature decreases from 50 °C, the apparent radius of gyration begins to increase, then decreases sharply and increases again, while p increases monotonously. For the lowest concentrations ($C <$ cac),

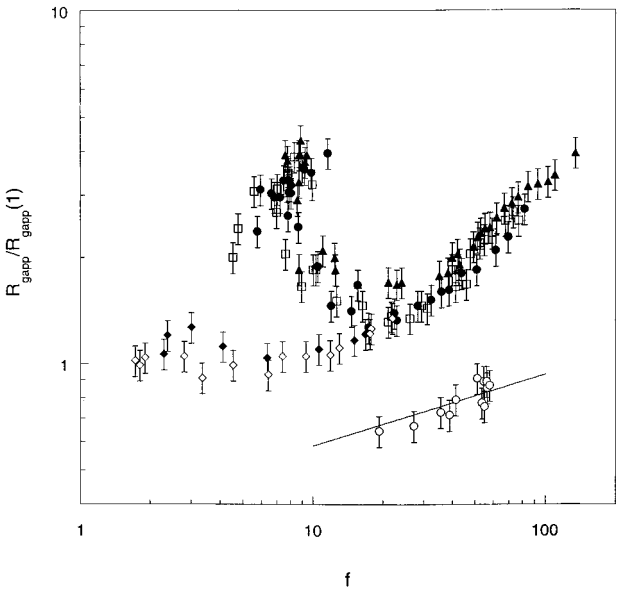

Figure 6. Variation of the reduced apparent radius of gyration $R_{gapp}(p)/R_{gapp}(1)$ as a function of twice the association number $f = 2p$. The symbol meaning is the same as in Figures 4 and 5. Increasing f corresponds to decreasing temperature. For comparison, hollow circles correspond to the variation of the apparent radius of gyration of diblock micelles (expressed in au for reasons of clarity). The line corresponds to the $p^{0.2}$ behavior expected for starlike micelles.

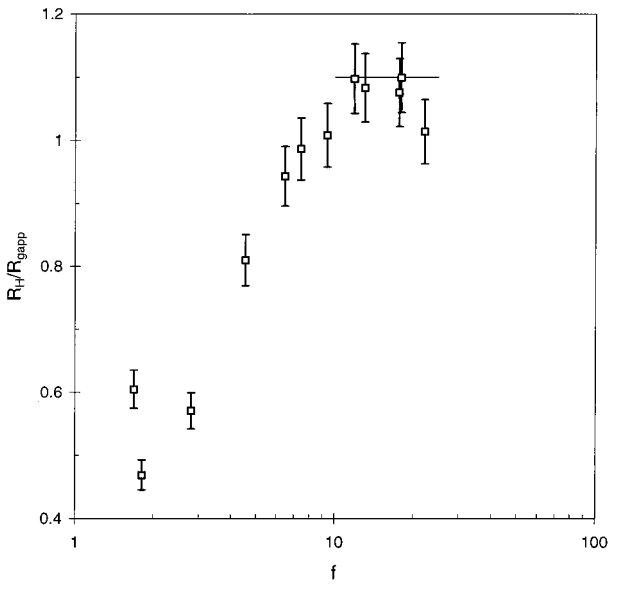

Figure 7. Ratio of the hydrodynamic radius to the radius of gyration of triblock copolymers aggregates as a function of the number $f = 2p$ of PS blocks per aggregate measured at $C = 8.9 \times 10^{-4}$ g/cm^3. The line corresponds to the mean value 1.1 $\pm$ 0.1 measured for the different concentrations.

above 20 °C the apparent radius of gyration remains constant and is equal to the one of free triblock copolymers in good solvent (260 Å, see the Table), below 20 °C it increases by a factor 1.3 while p increases by a factor of 5. This result clearly indicates the triblock aggregate compaction as the solvent selectivity increases.

In order to outline the aggregate compaction, the variation of the apparent radius of gyration R_{gapp} as a function of the number f of PS blocks per aggregate is plotted in Figure 6 for triblock copolymer. At low f values ($f < 20$) data behave differently depending on the concentration. For $C <$ cac, R_{gapp} is f independent for $f < 5$ and shows a $f^{0.2}$ compatible behavior for $8 < f < 20$. For $C >$ cac, the apparent radius of gyration R_{gapp} decreases abruptly as f increases. At high f values ($f >$ 20), the apparent radius of gyration increases with the association number, irrespective of the concentration. For $C >$ cac, triblock copolymers aggregates pass from a low density (high radius of gyration and small association number) to a higher density structure (lower radius of gyration and higher association number) for decreasing temperatures. However, in this high association number regime, the variation of the radius of gyration is larger than the $f^{0.2}$ behavior expected for spherical starlike micelles and actually observed for diblock copolymers (see Figure 6).

Another way to display the aggregate compaction is to consider the variation of the ratio R_H/R_{gapp} with the association number. This ratio reaches the constant value $R_H/R_{gapp} = 1.1 \pm 0.1$ for $p > 10$, irrespective of the concentration. As an example, this ratio measured for a given concentration, below the cac, is plotted in Figure 7. The ratio R_H/R_{gapp} is found to be comparable to the value of $(5/3)^{1/2}$ expected for dense spheres and measured on starlike polymers.[24] However, one has to keep in mind that R_{gapp} differs from the actual radius of gyration due to the difference of refractive index of the two blocks.

2.4. Small-Angle Neutron Scattering Measurements. Small-angle neutron scattering experiments were performed with the PACE and PAXY spectrometers in Saclay, France. Different configurations were used, allowing the q range 3×10^{-3} to 2×10^{-1} Å^{-1} to be covered, depending on the incident wavelength and on the distance between the sample and the multidetector. Water flow inside the sample holder allows temperature regulation with an accuracy of the order of 0.5 °C. Data treatment was done following ref 25.

2.4.1. Diblock Copolymers. For the diblock copolymers, two contrasts between polymer and solvent were used. First, using deuterated heptane, the form factor of the overall micelles was measured at low concentration ($C = 4.5 \times 10^{-3}$ g/cm^3) and room temperature. Second, the suitability of neutron scattering for contrast matching was used by mixing deuterated and non-deuterated heptane in such a proportion that the polyisoprene blocks were rendered invisible. In the latter case, because of the low scattered intensity, the polymer concentration was higher ($C = 10^{-2}$ g/cm^3) than in the former case. However, results obtained in both cases remain comparable because the association number of diblock micelles is concentration independent at room temperature for $C > 10^{-4}$ g/cm^3. In Figure 8 the scattered intensity per monomer measured in the first case, is plotted as a function of the transfer vector **q**. Neglecting micelle interactions the scattered intensity per monomer corresponds to the form factor of micelles. This form factor is quite reminiscent of the one predicted and observed for starlike polymers,[26] which exhibits a power law behavior characteristic of swollen polymers since the observation length scale q^{-1} is smaller than the size ξ of the largest blob ($q\,\xi > 1$) and a sharp decrease at $R^{-1} < q < \xi^{-1}$. These two features appear clearly in Figure 8 at high q ($q > 4 \times 10^{-2}$ Å^{-1}) and at low q ($q < 2 \times 10^{-2}$ Å^{-1}), respectively. At high q, the scattered intensity varies as $q^{-1.74}$, behavior attributed to the swollen corona of polyisoprene. As for the intermediate q range ($2 \times 10^{-2} <$ q (Å^{-1}) $< 4 \times 10^{-2}$), it exhibits a shoulder not present in the starlike polymer form factor. To confirm that this shoulder can be

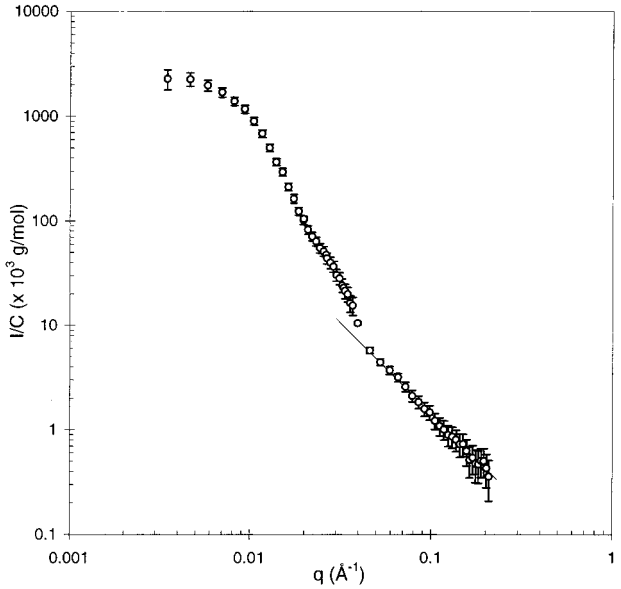

Figure 8. Small angle neutron scattered intensity per monomer I/C as a function of the transfer vector q, measured at room temperature for diblock copolymer micelles in deuterated heptane at a concentration of $C = 4.5 \times 10^{-3}$ g/cm^3. The line corresponds to the best power law fit for the high q range leading to an exponent equal to 1.74, not far from the value expected for swollen linear polymers.

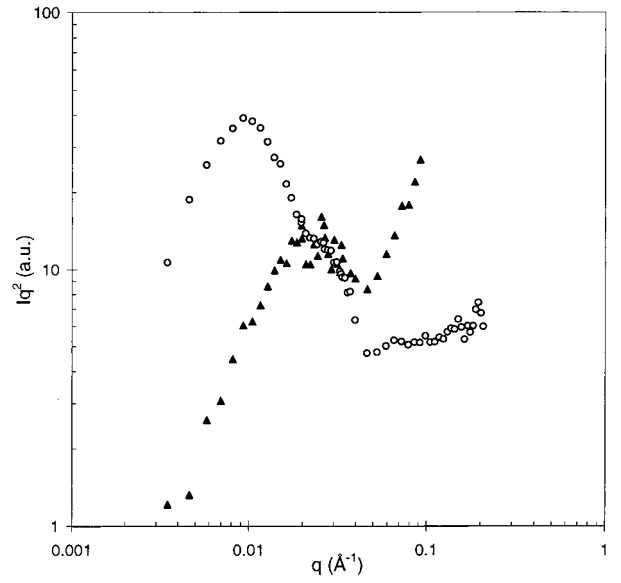

Figure 9. Neutron scattered intensity I multiplied by q^2 as a function of the transfer vector **q**. Hollow circles correspond to diblock copolymer micelles in deuterated heptane (as in Figure 8). Full triangles correspond to the diblock copolymer in a mixture of deuterated and nondeuterated heptane in order to hide the polyisoprene corona of the micelles. In the latter case, the maximum observed at $q = (2.3 \pm 0.1) \times 10^{-2}$ Å^{-1} allows us to estimate the radius of the core $R_{core} = 90$ Å. Comparison of both spectra allows us to attribute the scattered intensity shoulder at $2 \times 10^{-2} < q$ (Å^{-1}) $< 3 \times 10^{-2}$ to the core contribution of the overall micelle scattered intensity.

attributed to the polystyrene core, let us compare the intensities scattered by the overall micelles and by the core, respectively. As the overall micelles and the core have spherical shape, let us plot the product Iq^2 as a function of q which exhibits a maximum at $qR = 2.1$ for spheres of radius R. In Figure 9, one can see that the maximum observed at $q = (2.3 \pm 0.1) \times 10^{-2}$ Å^{-1} in the case for which only the core is visible coincides with the shoulder displayed when the overall micelle is

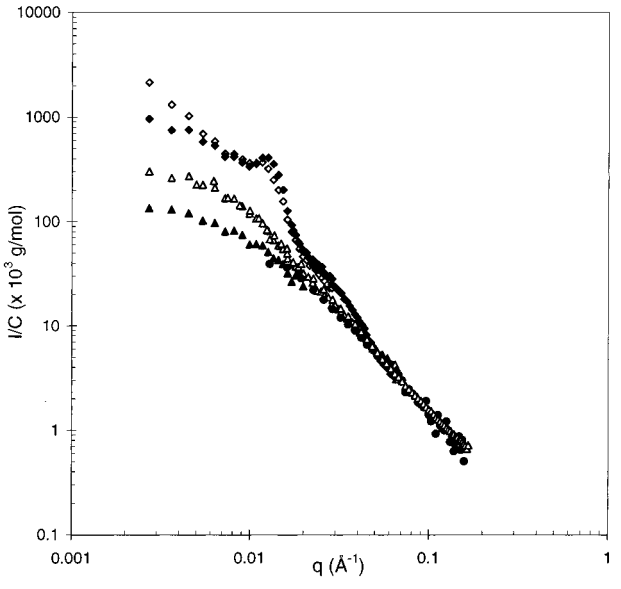

Figure 10. Concentration effect on the scattered intensity per monomer measured as a function of q for triblock copolymers: hollow symbols, $C = 1.4 \times 10^{-2}$ g/cm^3; full symbols, $C = 6.3 \times 10^{-4}$ g/cm^3; triangles, $T = 45$ °C; diamonds, $T = 13$ °C. At high temperature, the aggregation process induces an increase of the scattered intensity at low q, while at low temperature the scattered intensity at $q > 6 \times 10^{-3}$ Å^{-1} is insensitive to the increase of the association number with concentration. In particular, the spectra display maximums at the same positions irrespective of the concentration.

observed.[27] The radius of the core can thus be estimated as equal to $R_{core} = 90$Å. One can compare R_{core} to the end-to-end distance of the PS block assuming a gaussian conformation: $S = 6^{1/2} \times 0.3 \times M^{1/2} = 86$ Å. The polystyrene concentration inside the core is on the order of 50%, which is higher than the micelle internal concentration which is on the order of 10% as given in section 2.3.1.

Due to the contribution of the core to the scattered intensity, it is not possible from neutron scattering spectra to estimate the size ξ of the largest blob of the polyisoprene corona, as can be done for starlike polymers. However, for star polymers having a radius of gyration R_g, ξ is expected to scale as $R_g/f^{1/2}$, where f is the number of arms. Taking the hydrodynamic radius of micelles as equal to their overall radius, one can give a rough estimate of $\xi \approx (3/5)^{1/2} R_H/f^{1/2}$, leading to $\xi = 33$ Å which is consistent with the measured form factor of micelles (see Figure 8).

2.4.2. Triblock Copolymers. In deuterated heptane, triblock copolymers were studied at two concentrations: $C_1 = 1.4 \times 10^{-2}$ g/cm^3 and $C_2 = 6.3 \times 10^{-4}$ g/cm^3. The concentration C_1 is on the order of the overlap concentration of free triblock copolymers measured in a good solvent, whereas the concentration C_2 is below the cac. In Figures 10 and 11 the absolute scattered intensity per monomer is plotted as a function of the transfer vector q for the two concentrations at different temperatures (Figure 10) and compared to scattered intensity of diblock micelles (Figure 11).

At high temperature (45 °C, triangles) the q-dependent scattered intensity is characteristic of linear polymers. For the lowest concentration (full symbols) the intensity measured at the lower q value is consistent with the mass of free copolymers. Actually, the radius of gyration $R_{gapp}(1)$ of free copolymers determined by light scattering indicates that neutron scattering measurements were performed at $qR_{gapp}(1) > 0.9$. For the

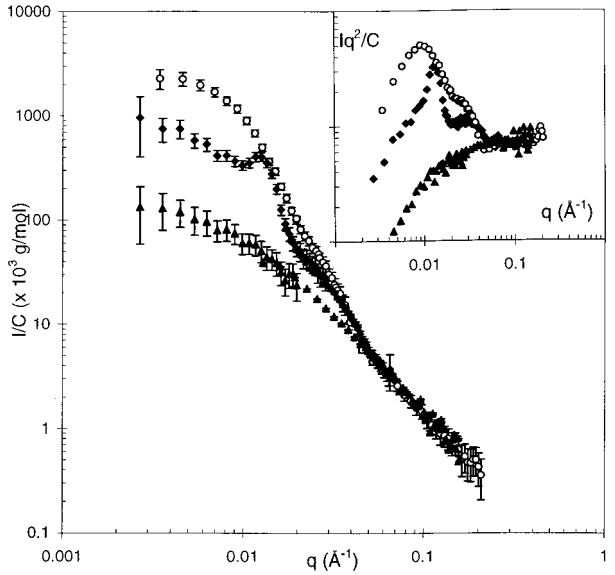

Figure 11. Small-angle neutron scattered intensity per monomers I/C vs the transfer vector **q** for triblock copolymers at two different temperatures compared to diblock copolymers at room temperature. The symbol meaning is the same as in Figure 8 and Figure 10. The triblock copolymer concentration is below the cac. Thus, only free copolymers are present in the solution at high temperature (full triangles). At low temperature, the intensity scattered by triblock aggregates shows a maximum at $q = 1.2 \times 10^{-2}$ Å^{-1} (full diamonds) and a shoulder at the same q position as the one observed for diblock micelles. This is highlighted in the inset where Iq^2/C (in au) is plotted as a function of q.

highest concentration (open symbols), the value of the scattered intensity at low q is sensitive to the association number of animals already reported.[12] At high q ($q > 4 \times 10^{-2}$ Å^{-1}) the scattered intensity remains temperature and concentration independent and merges with the one measured for free triblock copolymers and for diblock copolymer micelles (see Figure 11). This reveals the swollen conformation of copolymers at this length scale, whatever their state of association.

At low temperature (13 °C, diamonds), triblock copolymers present a scattered intensity shoulder at approximately the same q value as for diblock copolymers ($q = 3 \times 10^{-2}$ Å^{-1}, see Figure 11). This is an indication of the existence of a dense polystyrene core, as for diblock copolymer micelles. In the intermediate q range, the intensity scattered by triblock copolymers exhibits a maximum at $q^\dagger = 1.2 \times 10^{-2}$ Å^{-1}. As shown in Figure 10, this maximum appears at the same position irrespective of the concentration. Consequently, it corresponds to a characteristic length inside triblock aggregates rather than to aggregate interactions (as it is found for instance with diblock micelles[4] near C^*). In terms of distance, the position $q^\dagger$ of this maximum corresponds to a characteristic length $d = 2\pi/q^\dagger = 520$ Å. This distance may be compared to twice the hydrodynamic radius of diblock micelles $2R_H = 580 \pm 10$ Å. Note that taking into account the variation of the radius of the micelles with the mass of copolymers, $R_H \propto M^\nu$, gives $2R_H = 510$ Å for a half-triblock micelle having the same association number as diblock copolymers. Thus, this distance is compatible with the distance between two PS cores belonging to spherical flower micelles in contact. It is important to note that the solution at concentration C_1 is cloudy at $T = 13$ °C but it is not at $T = 16$ °C, however the q-dependent neutron scattering intensity measured at these two temperatures remains identical. This means that at short length scales the macroscopic dense phase present at 13 °C for this concentration and the aggregates at 16 °C are indiscernible.

In summary, diblock as well as triblock copolymers associate in dense micelles at low temperature. However, small-angle neutron scattering shows that triblock copolymers form micelle associations due to their ability to form bridges.

3. Theoretical Background and Discussion

Block copolymers are made of several sequences belonging to different chemical species. In a bad solvent for one of the species, A, and a good solvent for the other, B, polymer−solvent interactions dominate. The interfacial energy between the A blocks and the solvent acts as a driving force for aggregation of the copolymers. To describe theoretically the thermodynamics of this aggregation process, one has to take into account all the contributions which balance this driving force, such as the translational entropy loss and also terms linked to the aggregate geometry.

3.1. Interfacial Energy from Solubility Measurements. If free polymers and polymers associated in large aggregates are in equilibrium the chemical potentials of chains in these two phases are equal. The simplest case corresponds to homopolymers of the A species, for which there is a macrophase separation between a dilute phase at a monomer concentration C_S and a dense (semidilute or concentrated) phase at a concentration C_{SD}. The chemical potential μ_d of free chains is a sum of two terms accounting for the translational entropy per chain and for the free energy per chain. Assuming that polymer chains are moving in a continuous medium (or on a lattice having a unit cell dimension equal to the size a of monomers) rather than in a discrete medium (i.e., on a lattice having a unit cell dimension equal to the radius of gyration of polymer chains) the translational entropy is equal to $k \times \ln(C_S/(\rho_A N_A))$, where N_A is the degree of polymerization of the chains and $\rho_A = 1/a^3$ their density. Regarding the free energy, it can be written in terms of an effective interfacial tension γ_i between A monomers and solvent molecules. Taking chains in the dense phase as the reference state and assuming collapsed chains in the dilute phase this last term E_γ scales as

$$E_\gamma = \gamma_i N_A^{2/3} \tag{4}$$

The chemical potential of a chain in the dense phase is reduced to its entropy term: $\mu_{SD} = \ln(C_{SD}/(\rho_A N_A))$, leading to $\ln(C_S/\rho_A) = \ln(C_{SD}/\rho_A) - E_\gamma$. Since we are considering the case of a polymer−solvent system far below the Θ temperature, the logarithm of the volume fraction C_{SD}/ρ_A of the dense phase can be neglected compared to $\ln(C_S/\rho_A)$.[28] The effective interfacial tension γ_i per monomer can thus be deduced from the solubility measurements reported in Figure 1 on three different polystyrene samples having masses equal to 2.20×10^4, 1.16×10^4, and 7×10^3 g/mol. The ratio $\gamma_i = \ln(C_S/\rho_{PS})/N_{PS}^{2/3}$ is plotted in Figure 12. A single curve is obtained in agreement with the $N_A^{2/3}$ scaling of the interfacial free energy E_γ. From this figure and eq 4, E_γ can be evaluated for a given polystyrene block having a known molecular mass. For instance, for the diblock PS precursors E_γ is found to be equal to $13kT$ at 60 °C and, by extrapolation equal to $22kT$ at 20 °C.

3.2. Diblock Copolymers. In the case of the copolymer−solvent system studied here, light and small angle

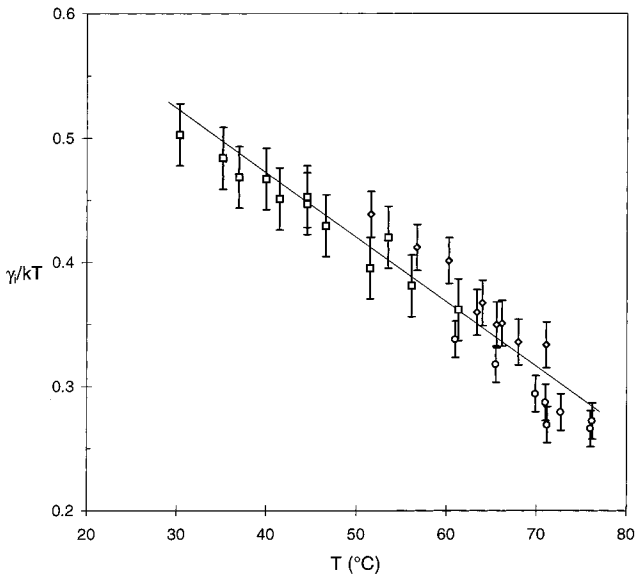

Figure 12. Effective interfacial tension γ_i per monomer deduced from solubility measurements reported in Figure 1: $\gamma_i/kT = \ln(C_S/\rho_{PS})/N_{PS}^{2/3}$ where C_S is the solubility, ρ_{PS} the density, and N_{PS} the degree of polymerization of polystyrene having a molecular mass equal to 7×10^3 (squares), 1.1×10^4 (diamonds) and 2.2×10^4 g/mol (circles). The line corresponds to the best linear fit: $\gamma_i/kT = (0.68 \pm 0.01) - (5.2 \pm 0.2) \times 10^{-3}T$ (°C).

neutron scattering results have shown that diblock copolymers aggregate in dense structures such as spherical micelles. Consequently, only this kind of structure will be considered in this part. The other structures which can be found for decreasing solvent selectivity will be discussed in a forthcoming paper.[2]

Spherical micelles are often described using a model of starlike polymers. This model considers a dense core made of the A blocks in a poor solvent condition and a swollen corona made of the B blocks. In this case, the optimum of the association number p corresponds to a balance between the interfacial energy gain $p^{-1/3}E_\gamma$ due to the association of A blocks and the osmotic energy loss E_{corona} due to the B-block concentration inside the corona. Classically, this last term is equal to kT per blob[5] and is expected to scale as $E_{corona}/p \propto p^{1/2} \ln(R_{micelle}/R_{core})$. The free energy per diblock copolymer chain inside one micelle is thus equal to

$$E_{Dib-Micelle} = p^{-1/3}E_\gamma + \frac{E_{corona}}{p} \qquad (5)$$

(throughout this section the energies are expressed in units of kT). In order to quantitatively check the agreement between theory and experiment, the prefactor of E_{corona} must be determined as it was done for E_γ. For large p values, the radius $R_{micelle}$ of the overall micelle varies as $p^{0.2}$ as for the starlike polymer,[23] whereas the radius of the core varies as $p^{1/3}$, leading to a negligible variation of the ratio $R_{micelle}/R_{core}$ with p (note that taking $R_{micelle}$ equal to the hydrodynamic radius measured by quasielastic light scattering and R_{core} measured by small angle neutron scattering, one obtains $R_{micelle}/R_{core} \cong 3$). The free energy per diblock copolymer chain in a micelle can thus be written as $E_{Dib-Micelle} = p^{-1/3}E_\gamma + Ap^{1/2}$, where the constant A can be determined by minimizing $E_{Dib-Micelle}$ with respect to p and knowing that for $T = 20$ °C, one has $E_\gamma \cong 22kT$ and $p \cong 50$ (averaged value for the three highest concentrations reported in Figure 3). One finds $E_{corona}/p = 0.5p^{1/2}$. To account for the variation of the corona energy with the mass of the PI-blocks, E_{corona} can be written as

$$\frac{E_{corona}}{p} = 0.5p^{1/2}\left(1 + \ln\left(\frac{M_{PI}}{M_{PI-Diblock}}\right)^\nu\right) \qquad (6)$$

where $\nu = 0.588$ is the excluded volume exponent and $M_{PI-Diblock} = 0.7 \times 8.0 \times 10^4$ g/mol is the mass of the PI part of the diblock which allowed us to determine the prefactor $A = 0.5$. The previous expression for E_{corona} and the known value of $E_\gamma(T)$ allow us to minimize $E_{Dib-Micelle}$ with respect to p at different temperatures and then to compare the theoretical variation of p with the experimental behavior (full line in Figure 3). At low temperature ($T > 25$ °C), one can see a good agreement between the experimental values and the theoretical curve, whereas at high temperature experimental values are smaller than expected. In other words, the above theoretical description accounts for the diblock copolymers micellization as long as association numbers measured in the concentration plateau are concerned. This is not surprising because such a theoretical description only predicts the concentration-independent association number. The association number increases over two decades in concentration for small values of p, a feature which remains still puzzling. Note that such a minimization of eq 6 leads to a free energy per chain in micelles on the order of $10kT$ at 20 °C.

3.3. Triblock Copolymers. In the previous sections, basic energy considerations allowed us to account for the diblock micelles conformation and their growth. In the case of triblock copolymers, the experiments revealed a change in the aggregate conformation which passes from animal-like to connected micelles for decreasing temperature. In order to discuss these experimental results, in the following, the conformation of free chains will be first considered. It will be shown that for triblock aggregation the entropy of the chain conformation is a term which plays a major role. The free energy for the flower structure will be examined. The numerical values for the energies involved in this conformation indicate that the flower structure is unfavorable at high temperature. Then a tentative theoretical description of the observed aggregate conformation will be given: at high temperature in order to account for the animal structure and at low temperature for the connected micelles which are found experimentally.

3.3.1. Conformation of Free Copolymer Chains. Triblock copolymers can adopt either a dumbbell or a ring conformation, depending on the balance between the interfacial energy gain and the entropy loss corresponding to the association of the two terminal blocks. For the dumbbell conformation one has

$$E_{Dumbbell} = 2E_\gamma \qquad (7)$$

while for the ring conformation

$$E_{Ring} = 2^{2/3}E_\gamma + E_{loop} \qquad (8)$$

In the latter expression, the first term corresponds to the interfacial gain, whereas the second term corresponds to the entropy loss due to the backfolding of the middle block B. Usually[10,11] E_{loop} is written in the form $^3/_2\beta \times \ln(N_B)$. In the case of pointlike A blocks, the factor $3\beta/2$ depends on the solvent quality for the B block

(i.e. Gaussian or swollen conformation) and is equal to $3\nu + \gamma - 1$, where γ and ν are the corresponding critical exponents.[29] For excluded volume chains[30] $\nu = 0.588$ and $\gamma = 1.161$ lead to $3\beta/2 \cong 2$ ($\beta \cong 1.3$). This logarithmic form of E_{loop} has been extended[11] to the general case with a phenomenological exponent β depending on N_A. However, we propose the following expression based on scaling considerations (see Appendix I)

$$E_{loop} = (3\nu + \gamma - 1)\ln(N_B) - \left(\frac{\gamma - 1}{\nu}\right)\ln(R_A/a) \quad (9)$$

for $R_A/R_B << 1$, where R_A is the radius of the A block globule, R_B the one of the swollen B block, and a the monomer size. The values of E_γ, deduced from the polystyrene solubility measurements, show that in the temperature range investigated, E_{Ring} is higher than $E_{Dumbbell}$ by almost $8kT$, assuming an A block concentration on the order of 1 in the globule. Therefore, the dumbbell conformation is always the most favorable.[31]

3.3.2. Triblock Aggregate Structures. For triblock copolymer aggregates, one may wonder whether the conformation entropy term prevents copolymers from forming flowerlike micelles as it prevents free copolymers from adopting a ring shape. To do such an evaluation, one needs to compare the free energy of these micelles to the one of other aggregate structures as for example "stripped flowers" for which chains do not go back to the core of the micelles.

The flower structure implies an energy having an expression comparable to eq 5 with a core and a corona made of $2p$ "half triblock chains". In order to obtain such a micelle, let us first cut the triblock copolymer in two equal parts. This leads to an excluded volume energy loss equal to $(\gamma - 1)(2\ln(N_B/2) - \ln(N_B))$. In addition, compared to diblock micelles, the corona term is supplemented with the constraint that the arms should meet two by two, so that the initial triblock copolymer is restored. We show in Appendix II that this constraint results in a energy shift per chain with respect to that of the corresponding diblock micelle:

$$E_{Flower} = 2E_{Dib-Micelle}(2p) - (\gamma - 1)\ln\left(\frac{N_B}{4}\right) + \frac{3}{2}\beta\ln(g_{max}) \quad (10)$$

where $3\beta/2 = 3\nu + (\gamma - 1)$ and $g_{max} \cong N_B/(2p)^{1/2}$ is the number of monomers belonging to the outer blob of the corona.

Let us call stripped flower a triblock micelle for which only one extremity of a given copolymer participates to the core. In this case, there is no loop entropy but an interfacial energy loss due to the copolymer extremity which does not join the core. In addition, the core and the corona contain only p chains but the mass which has to be considered is M_{PI} instead of $M_{PI}/2$. The free energy per chain is thus equal to

$$E_{Stripped} = (p^{-1/3} + 1)E_\gamma + \frac{E_{corona}(p, M_{PI})}{p} \quad (11)$$

These micelle free energies per chain can be compared by minimizing eq 10 and 11 with respect to p. In the case of the triblock studied in this paper, this can be done at different temperatures using Table 1, eqs 4 and 6, and Figure 12. The results are plotted in Figure 13 and discussed in section 3.3.3.

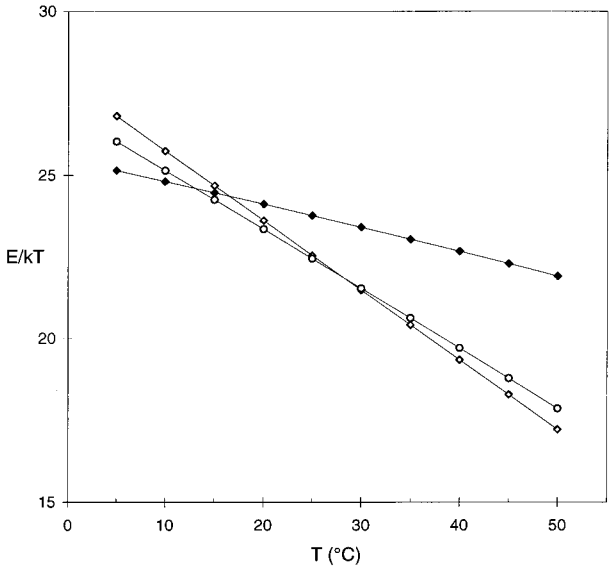

Figure 13. Free energy per chain as a function of the temperature for "flowers" (full symbols) obtained by minimization of eq 10, for "stripped flowers" (open circles) obtained by minimization of eq 11 and for "superchains" (open diamonds) from asymptotic behavior of eq 12.

At high temperatures, it was shown that triblock copolymers do not associate in dense structures but rather in loose, polydispersed and presumably branched aggregates. It is not as easy as for micelles to write down the free energy of such aggregates, and only very approximate models can be considered. Let us take as a rough model the "copolymer superchains" made of n end-to-end connected chains. This is quite similar to equilibrium polymerization[32,33] of living polymers such as those encountered in sulfur. When a chain is added to a superchain, there is an interfacial energy gain due to the connection of two terminal blocks, but an entropy loss due to the excluded volume interactions. The free energy per triblock chain of these superchains can thus be written as

$$E_{Superchain} = 2^{2/3}E_\gamma + \frac{(2 - 2^{2/3})}{p}E_\gamma + \frac{(\gamma - 1)}{p}\ln\left(\frac{N_B^{(p-1)}}{p}\right) \quad (12)$$

Once such equilibrium polymerization is allowed, there is no minimum value for the free energy $E_{Superchain}(p)$. Indeed, it has been shown that the mass distribution of these superchains is a power law of the form $p^{\gamma-1}$ with an exponential cutoff for large values of p. In our case, it would be interesting to take into account the possibility of branching. However, for our purpose let us just neglect the two last terms in eq 12 and consider only the first term which is p independent. This term corresponds to the free energy per unit length of the superchains and thus to the critical chemical potential of aggregation[34] at which the mass distribution becomes infinite. Comparison of $E_{superchain}$ with the minimum value of E_{Flower} (eq 10) and $E_{stripped}$ (eq 11) is made in Figure 13.

3.3.3. Discussion. From the comparison of the free energy per chain for the different aggregate structures (see Figure 13), one finds that at low temperatures ($T < 15$ °C) the flower structure is favorable whereas it is not at high temperatures ($T > 15$ °C). Thus flowers cannot be observed in this temperature regime because

there exist other conformations having much lower free energy. The same figure shows that, in the temperature range considered, the free energy per chain for the stripped flower and the superchain structures are of the same order of magnitude. Actually these two conceivable conformations constitute boundary cases, and the aggregate structure at high temperature is presumably intermediate: something like branched superchains which were called "animals" in the Experimental Results section. The transition temperature from animal to flower conformations, which is found at a temperature on the order of 15 °C, is in reasonable agreement with the aggregate compaction shown in Figure 5, for example. Note that, from Figure 13, a transition from a superchain to a stripped flower conformation could be also considered at a temperature between 25 and 30 °C. This transition implies an aggregate compaction, as well, and leads to a broadening of the transition temperature zone where aggregates pass from a loose to a compact structure.

As the temperature decreases, it was shown in the previous sections that dense structures such as spherical micelles appear. Compared to diblock copolymers the ability of triblocks to form bridges and then to interconnect micelles has been already reported from a theoretical point of view.[8,14] Starting from flower triblock micelles already present in the solution, Semenov et al.[8] consider that association of isolated flowers can be considerably slowed down due to the energy barrier encountered by one A-block going out the core and passing through the corona of one micelle. Isolated flowers are thus metastable structures, more or less quenched by this energy barrier. It is clear that starting from another isolated aggregate structures, such as stripped flower or superchain, would reduce this energy barrier. Following these authors, triblock micelle association can be viewed as a phase separation. In such a case, in the temperature range which is favorable for the observation of flowerlike micelles, their association cannot be avoided, leading to infinite clusters. However, it is important to point out that this concept does not suit the experimental results reported in this paper, because of the finite size and of the reversible behavior of the micelle association which are observed. As for the case of superchains, cyclisation and branching between micelles may prevent infinite clusters to appear. Note that the results obtains by Monte-Carlo simulations[35] performed on equivalent systems are in better agreement with our observations than the above theoretical approach.

In this paper we focused more primarily on the change of the triblock aggregate structure in dilute solutions as the temperature is decreased. It was shown in a previous paper,[36] that as the concentration increases and reaches the overlap concentration, the system forms a body-centered cubic structure, whose characteristics, such as the lattice parameter and the plateau elastic modulus, are independent of temperature. This means that the structure of the aggregates formed in dilute solution does not influence the properties of the semidilute solutions.

4. Conclusion

In a previous paper,[12] it has been shown that under weak segregation conditions (high temperature) telechelic triblock copolymers in dilute solution associate in loose, polydispersed, and branched aggregates, which were called animals. This paper presents experimental evidence for an aggregate compaction as the segregation effect becomes stronger (decreasing temperature). Dense structures are thus obtained. However, small-angle neutron scattering experiments show that, instead of isolated flowerlike micelles, one always obtains micelle associations. Such associations were theoretically expected and are due to the ability of telechelic copolymers to form bridges. They can be viewed as the precursor of the macrophase which is responsible of the cloudy point in these systems. But in our case, they correspond to stable rather than metastable structures. Theoretical investigations of these aggregates and of the animals formed at high temperatures remain to be done. Nevertheless, the experimental determination of the interfacial tension between the solvent and the block in a bad solvent condition (PS) used conjointly with the study of diblock micelles allows the energy terms involved in the triblock aggregation process to be quantified. Then using crude models, a transition from animals to flowers is predicted to occur as the temperature is decreased, in agreement with the experimental results reported here.

Acknowledgment. We would like to thank J. François, P. Schleger, and O. V. Borisov for the PS fraction determination, correcting the English, and interesting discussions.

Appendix I

Here we evaluate for ABA triblock copolymers, $E_{loop} = \ln(\Omega_D/\Omega_R)$ as a function of N_B and $R_A \cong N_A^{1/3} C_{SD}^{-1/3}$ (radius of an A globule), where Ω_D and Ω_R are the total number of states in the dumbbell and ring conformation, respectively. In Ω_R one must sum over the two end points lying on a shell of radius $2^{1/3}R_A$ and thickness a. For Ω_D, each end point lies on shell of radius R_A and furthermore one must integrate over all relative positions of the two "balloons" of the dumbbell. This is rather complicated but can be rapidly estimated by scaling considerations.

(1) For $R_A = a$, E_{loop} is simply related to the return probability of a swollen chain:[37]

$$E_{loop}|_{R_A=a} = (3\nu + \gamma - 1)\ln N_B$$

(2) For $R_A \to \infty$, Ω_R is given by

$$\Omega_R \cong (R_A/a)^2 z^{N_B} N_B^{\gamma_{1,1}-1}$$

according to the theory of critical phenomena near a planar surface (for a review see, e.g., ref 39). The dumbbell problem is that of a chain grafted between two parallel planes with a spacing D.

$$\Omega_D \cong (R_A/a)^4 \int_0^\infty \mathrm{d}D\, z^{N_B} N_B^{\gamma_{1,1}-1} f_\Omega(D/N_B^{\nu})$$

so that

$$E_{loop}|_{R_A\to\infty} = \ln[(R_A/a)^2 N_B^{\nu}]$$

in kT unit.

(3) In the intermediate case, a scaling behavior is expected

$$E_{loop} = \ln[N_B^{\nu} g(R_A/aN_B^{\nu})(R_A/a)^2]$$

with $g(x) = O(1)$ for $x \to \infty$ and $g(x) \cong x^{-(2\nu+\gamma-1)/\nu}$ for $x \to 0$. For $R_A \ll R_B$, with $R_B = R_B = aN_B^{\nu}$:

$$E_{loop} = (3\nu + \gamma - 1)\ln N_B - \left(\frac{\gamma - 1}{\nu}\right)\ln(R_A/a)$$

Note that this result holds whether we chose the core as impenetrable (realistic situation) or not. It is also in contradiction with the proposal by Wang et al.:[11] $E_{loop} = {}^3/_2\beta(R_A)\ln N_B + ...$, where $\beta(R_A)$ would be a nonuniversal exponent.

Appendix II

In order to compare micellization of a triblock ABA copolymer with that of a diblock AB chosen as the half of the triblock, we compute the difference between the free energy of a flower micelle made of p triblocks and that of a micelle containing $2p$ diblocks. Let us denote by Δ this difference divided by p. One can reasonably expect that the core and the interfacial region are identical in both cases, so that $p\Delta$ is the energy difference coming from the corona. We consider dense micelles (i.e., area per head much smaller than the square radius of B). The corona is dominated by monomer−monomer repulsion, so that the B segments starting out at the surface of the core are stretched and in both cases display the blob picture suggested by the Daoud−Cotton model.[23] Following Alexander−de Gennes, to a good approximation, we can assume that each end point for a diblock and each midpoint for a triblock lies in the external blob layer. Then Δ reflects the energy difference between the external blobs in the diblock case which are independent and those in the triblock case in which the sequences in neighboring blobs are linked two by two. External blobs have a number of monomers g_m and a linear size $\xi_m \sim g_m{}^{\nu}$. For one sequence of length g_m with one end fixed and the other free, the configuration number is[37]

$$Z(g_m) = z^{g_m} g_m{}^{\gamma-1}$$

For one sequence of length $2g_m$ and ends at points $\mathbf{r}_1$ and $\mathbf{r}_2$:

$$Z(\mathbf{r}_1 - \mathbf{r}_2, 2g_m) = Z(2g_m)\frac{1}{(2g_m)^{3\nu}} f\left(\frac{|\mathbf{r}_1 - \mathbf{r}_2|}{(2g_m)^{\nu}}\right)$$

For comparison between the diblock and triblock configurations one sets $|\mathbf{r}_1 - \mathbf{r}_2| \cong \xi_m$ on the average so that

$$\Delta = -\ln\left(\frac{Z(\xi_m, 2g_m)}{Z(g_m)^2}\right) = (3\nu + \gamma - 1)\ln(g_m) \quad \text{(A1)}$$

Note that an additional combinatorial term should be included in Δ coming from the different ways of linking the blobs two by two. This is the dimer problem on a lattice of $2p$ points, the total entropy of which is proportional to $2p$ and thus negligible. Since $g_m \cong N_B/p^{1/2}$, eq A 1 agrees with the theory of critical exponents of general polymer networks.[38] From Duplantier's work, one can compare a star polymer ($2p$ arms) and a flower polymer (p petals): the asymptotic behavior when $N \to \infty$ of the free energy difference is $p(3\nu + \gamma - 1)\ln(N)$.

For the limiting case of a planar brush ($R_{core} \to \infty$) made either of diblock or triblock copolymers the blob mass is a constant $g \sim \sigma^{-1/2\nu}$, where σ is the surface density of chains. Here eq A1 can be obtained through a general scaling argument as shown below. The entropy difference per triblock chain between the two cases is of the form $-k\Delta(\sigma, N_B)$. For σ much less than the overlap density $\sigma^* = 1/R_B{}^2$ ("mushroom" regime)

$$\Delta = -\ln\left(\int d^2\mathbf{r} \times Z(\mathbf{r}, N_B)\right) + 2\ln Z(N_B/2) + \ln(\sigma a^2/2) - 2\ln(\sigma a^2)$$

which yields the suggested form for the general situation:

$$\Delta(\sigma, N_B) = (\nu + \gamma - 1)\ln N_B - \ln \sigma a^2 + \ln\left[f\left(\frac{\sigma}{\sigma^*}\right)\right]$$

For $\sigma \gg \sigma^*$, Δ must be independent of N_B which yields

$$\Delta(\sigma, N_B) = -\left(\frac{3\nu + \gamma - 1}{2\nu}\right)\ln \sigma = (3\nu + \gamma - 1)\ln g$$

One could also take into account the impenetrable character of the grafting surface and use the corresponding surface exponents:

$$Z(N_B) = z^{N_B} N_B{}^{\gamma_1 - 1}$$

$$\int d^2\mathbf{r} \times Z(\mathbf{r}, N_B) = z^{N_B} N_B{}^{\gamma_{1,1} - 1}$$

However, the scaling relation[39] $2\gamma_1 - \gamma_{1,1} = \gamma + \nu$ leads to an unmodified result.

References and Notes

(1) Tuzar, Z.; Kratochvil, P. *Surf. Colloid. Sci.* **1992**, *15*, 1.
(2) Adam, M.; Lairez, D.; Raspaud, E.; Carton, J.-P. Manuscript in preparation.
(3) Cogan, K. A.; Gast, A. P.; Capel, M. *Macromolecules* **1991**, *24*, 6512.
(4) Adam, M.; Carton, J.-P.; Corona-Vallet, S.; Lairez, D. *J. Phys. II Fr.* **1996**, *6*, 1781.
(5) Halperin, A. *Macromolecules* **1987**, *20*, 2943.
(6) Leclerc, E.; Calmettes, P. *Phys. Rev. Lett.*, **1997**, *78*, 150.
(7) Chevillard, C.; Axelos, M. A. V. *Colloid Polym. Sci.* **1997**, *275*, 537.
(8) Semenov, A. N.; Joanny, J.-F.; Khokhlov, A. R. *Macromolecules* **1995**, *28*, 1066.
(9) Halperin, A. *Macromolecules* **1991**, *24*, 1418.
(10) ten Brinke, G.; Hadziioannou, G. *Macromolecules* **1987**, *20*, 486.
(11) Wang, Y.; Mattice, W. L.; Napper, D. H. *Macromolecules* **1992**, *25*, 4073.
(12) Raspaud, E.; Lairez, D.; Adam, M.; Carton, J.-P. *Macromolecules* **1994**, *27*, 2956.
(13) Stauffer, D. *J. Phys. Stat.* **1978**, *18*, 125.
(14) Borisov, O. V.; Halperin, A. *Macromolecules* **1996**, *29*, 2612.
(15) Brown, W.; Schillen, K.; Almgren, M.; Hvidt, S.; Bahadur, P. *J. Phys. Chem.* **1991**, *95*, 1850.
(16) Yang, Y.-W.; Yang Z.; Zhou, Z.-K.; Attwood, D.; Booth, C. *Macromolecules* **1996**, *29*, 670.
(17) Maechling-Strasser, C.; François, J.; Clouet, F.; Tripette, C. *Polymer* **1992**, *33*, 627.
(18) In ref 12, the weight fraction of PS was given as equal to 30%. In this paper, the reported value was kindly measured by J. François using UV spectroscopy.
(19) Luzzati, S.; Adam, M.; Delsanti, M. *Polymer* **1986**, *27*, 834. Adam, M.; Delsanti, M.; Munch, J.-P.; Durand, D. *J. Physique* **1987**, *48*, 1809.
(20) Benoit, H.; Leng, M. *Ind. Plast. Mod.* **1960**, *12*.
(21) Cotton, J.-P.; Benoit, H. *J. Phys. Paris* **1975**, *36*, 905.
(22) Adam, M; Fetters, L. J.; Graessley, W. W.; Witten, T. A. *Macromolecules* **1991**, *24*, 2434.
(23) Daoud, M.; Cotton, J.-P. *J. Phys.* **1982**, *43*, 531.
(24) Roovers, J.; Zhou, L.-L.; Toporowski, P. M.; van der Zwan, M.; Iatrou, H.; Hadjichristidis, N. *Macromolecules* **1993**, *26*, 4324.
(25) Cotton, J.-P. In *Neutron, X-ray and light scattering*; Linder,P., Zemb, Th., Eds., North-Holland: Amsterdam, 1991; pp 3−31.
(26) Adam, M.; Lairez, D. *Fractals* **1993**, *1*, 149.
(27) At $q > 4 \times 10^{-2}$ Å^{-1}, for the overall micelles the product Iq^2 increases because of the $q^{-1.74}$ dependence of the scattered intensity. For the measurement performed with a hidden

corona, the increase of the product Iq^2 in this q range is not significant and only reflects that the scattered intensity is on the order of the incoherent scattering.
(28) In part 2.4 the concentration C_{SD} is estimated to be on the order of 50% inside the core of diblock micelles.
(29) des Cloizeaux, J.; Jannink, G. in *Les polymères en solution*; Les Editions de Physique: Paris, **1987**; pp 53 and 108.
(30) Le Guillou, J. C.; Zinn-Justin, J. *Phys. Rev. Lett.* **1977**, *39*, 95.
(31) Since the description of micelles having a small association number is still questionable (see section 3.2), the same approach as applied to free triblock conformations may be too crude.
(32) Petschek, R. G.; Pfeuty, P.; Wheeler, J. C. *Phys. Rev. A* **1986**, *34*, 2391.
(33) Cates, M. E. *J. Phys. Fr.* **1988**, *49*, 1593.
(34) Izzo, D.; Marques, M. *Macromolecules* **1993**, *26*, 7189.
(35) Nguyen-Misra, M.; Mattice, W. L. *Macromolecules* **1995**, *28*, 1444.
(36) Raspaud, E.; Lairez, D.; Adam, M.; Carton, J.-P. *Macromolecules* **1996**, *29*, 1269.
(37) de Gennes, P.-G. *Scaling concepts in Polymer physics*; Cornell University Press: Ithaca, NY, 1979.
(38) Duplantier, B. *J. Stat. Phys.* **1989**, *54*, 581.
(39) Binder, K., In *Phase transitions and critical phenomena*, Domb, C., Lebowitz, J. L., Eds.; Academic Press: London, 1983; Vol. 8.

MA970666M